Supporting Information

Fluorescent nanofibrillar hydrogels of carbon dots and cellulose nanocrystals and their biocompatibility

Bowen Sui,[†] *Yuping Zhang,*[†] *Lei Huang,*[‡] *Yixin Chen,*[†] *Daowei Li,*[*,‡] *Yunfeng Li,*[*,†] *Bai Yang*[†]

[†]State Key Laboratory of Supramolecular Structure and Materials, College of Chemistry, Jilin University, Changchun, 130012, P. R. China.

[‡]Jilin Provincial Key Laboratory of Tooth Development and Bone Remodeling, Hospital of Stomatology, Jilin University, 1500 Qinghua Road, Changchun, 130021, P. R. China

*E-mail: yflichem@jlu.edu.cn;

jluldw@jlu.edu.cn

Supporting Information Contents:

Number of pages: 21

Number of figures: 15

Number of tables: 3

Experimental Section

Preparation of CNCs/PEI Suspensions. The mixed CNCs/PEI suspensions with C_{total} =7.7 wt % and 11.3 wt %, and weight ratios of CNCs to PEI, R=10, 5, 2, 1 and 0.5 were prepared according to the Table S1. For example, at C_{total} =7.7 wt % and R=10, 31.731 g 10.4 wt % suspension of CNCs and 0.330 g PEI were dissolved in 15.130 g DI water. The mixed aqueous suspensions were vortexed for 2 min and left for 10 hours to make PEI fully dissolved. The mixed suspensions were vortexed for 2 min again before use.

Characterization of the CNCs and CDs. The morphology of CDs was measured by using Transmission Electron Microscopy (TEM). 2 μL of the solution obtained by dialysis of nanofibrillar hydrogels in water was drop-casted on an ultrathin carbon film at room temperature. JEM-2100F electron microscope was used to obtain TEM images of CDs at 200 kV with a CCD camera. The obtained images were analyzed by using a software ImageJ. To suppress CNC aggregation, a dilute 0.01 wt % suspension of CNCs was drop-casted on a grid that was treated by oxygen plasma for 10 s. The TEM images of CNCs were obtained using a Hitachi HT7700 Transmission Electron Microscope at 85 kV. Moreover, the CNCs were measured by using Atomic Force Microscopy (AFM). 300 μL of 0.01 wt % CNCs suspension was spin-coated on a quartz substrate at 2000 rpm for 1 min. AFM images were all captured by the Bruker's Dimension FastScan Atomic Force Microscope under ambient condition. X-ray Photoelectron Spectroscopy (XPS) of CDs was investigated by using ESCALAB 250 spectrometer with a mono X-Ray source Al Kα excitation (1486.6 eV). Binding energy calibration was based on C1s at 284.6 eV.

Photoluminescence characterization. Photoluminescence (PL) spectra of the nanofibrillar hydrogels, pure CNCs hydrogels, 7.7 wt % suspension of CNCs, the mixed aqueous suspensions of CNCs and PEI, and CDs solution obtained by dialysis were performed on a RF-5301 PC spectrophotometer (Shimadzu). For the PL measurement of hydrogels, a slide of hydrogel with thickness of ~2 mm was cut by a surgical blade and adhered to a glass slide.

Characterization of Fourier Transform Infrared Spectroscopy.

Infrared spectra of CNCs, PEI, and the lyophilized hydrogels were recorded using an attenuated total reflectance Fourier transform infrared spectroscopy (ATR-FTIR, Thermo Fisher Scientific Nicolet iS10, Thermo Fisher Scientific Smart iTR* ATR with a diamond crystal). FTIR spectra of CDs was collected by Fourier transform infrared spectrometer

(VERTEX 80V, Brucker). All spectra were recorded between 4000 and 400 cm^{-1} with a resolution of 4 cm^{-1} and 32 scans.

Characterization of X-ray Diffraction.

X-Ray diffraction (XRD) analysis of CNCs and the lyophilized hydrogels was performed by X-ray diffractometer, Rigaku SmartLab 3, using a nickel-filtered Cu Kα radiation and the data was collected from 5° to 50°.

Dynamic light scattering (DLS).

The hydrodynamic diameters of CNCs and the zeta potential measurements of CNCs were conducted on a Malvern Nano-ZS Zetasizer at 25 ℃. The DLS measurement was carried out on the diluted suspensions with no pH adjustment. Three measurements were carried out with a delay of 60 s for equilibration time. The hydrodynamic diameter of CNCs was 137.5 ± 0.5 nm.

Table S1. The formula of CNCs/PEI suspensions for preparation of nanofibrillar hydrogels.

	***R*=10**		***R*=5**		***R*=2**		***R*=1**		***R*=0.5**	
	7.7%	**11.3%**	**7.7%**	**11.3%**	**7.7%**	**11.3%**	**7.7%**	**11.3%**	**7.7%**	**11.3%**
10.4 wt % CNCs / g	31.731	44.429	29.087	42.308	23.269	34.269	16.923	25.385	11.635	17.769
PEI / g	0.330	0.462	0.605	0.88	1.210	1.782	1.760	2.640	2.420	3.696
DI water / g	15.13	0	17.499	3.538	22.711	11.259	27.077	18.701	33.135	27.597

Table S2. Histological grading scale for inflammatory immune response

(1) Capsule quality	score
Capsule is fibrous, mature, not dense, resembling connective or fat tissue in the non-injured regions	5
Capsule tissue is fibrous but immature, showing fibroblasts and little collagen	4
Capsule tissue is granulous or dense, containing mainly fibroblasts and some inflammatory cells	3
Capsule tissue is granulous or dense, containing both fibroblasts and many inflammatory cells	2
Capsule consists of masses of inflammatory cells with little or no signs of connective tissue organization	1
Cannot be evaluated because of infection or other factors not necessarily related to the material	0
(2) Capsule thickness	score
1−4 fibroblasts	5
5−9 fibroblasts	4
10−30 fibroblasts with few inflammatory cells	3
10−30 containing both fibroblasts and inflammatory cells	2
10−30 inflammatory cells with few fibroblasts	1
not applicable	0
(3) Cell infiltration	score
Fibroblasts contact the implant surface without the presence of macrophages or leucocytes	4
Scattered foci of macrophages and leucocytes are present	3
One layer of macrophages and leucocytes are present	2
Multiple layers of macrophages and leucocytes present	1
Cannot be evaluated because of infection or other factors not necessarily related to the material	0

Table S3. Histological grading of different groups of hydrogels after 10 and 20 days subcutaneous implantation.

Day	Score	*R*=10	*R*=5	*R*=2	*R*=1	*R*=0.5
10	Capsule quality	1.2±0.4	1.2±0.4	2.0±0	2.8±0.4	3.0±0
	Capsule thickness	1.0±0	1.2±0.4	2.2±0.4	3.0±0	3.0±0
	Cell infiltration	1.0±0	1.0±0	2.4±0.5	2.8±0.4	2.8±0.4
20	Capsule quality	1.0±0	1.0±0	2.0±0	2.6±0.5	2.6±0.5
	Capsule thickness	1.2±0.4	1.2±0.4	1.8±0.4	2.6±0.5	2.6±0.5
	Cell infiltration	1.0±0	1.0±0	1.6±0.5	2.2±0.8	2.4±0.9

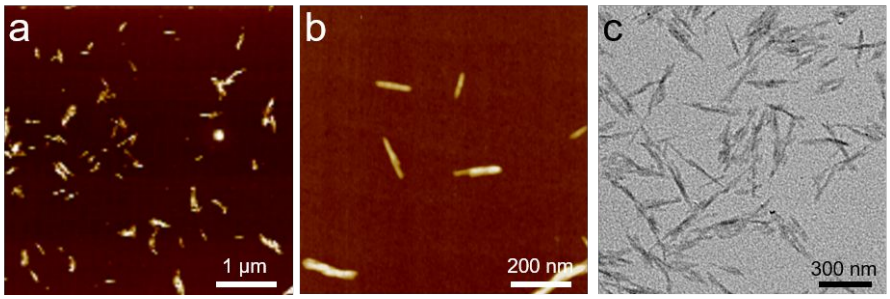

Figure S1. AFM images (a and b) and TEM (c) images of CNCs.

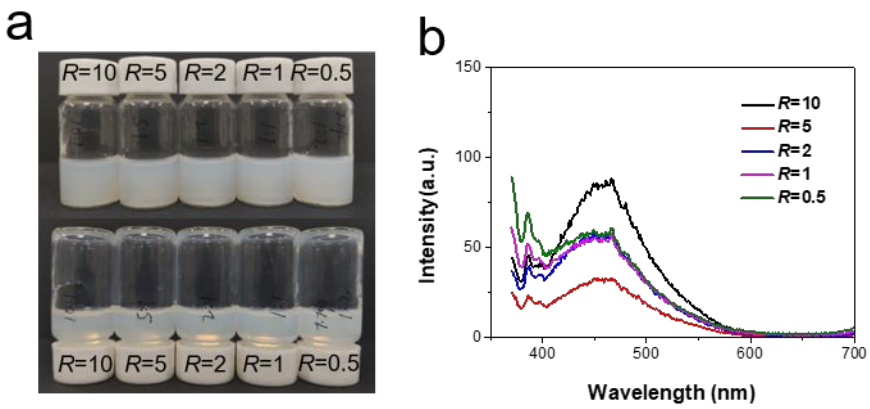

Figure S2. (a) Photos of 7.7 wt % mixed suspension of CNCs and PEI in glass vials without occurring of gelation for 30 days. (b) The PL spectra of the 7.7 wt % mixed suspensions of CNCs and PEI with different *R* at λ_{ex} = 360 nm. Both slit widths at excitation and emission were set at 3 nm.

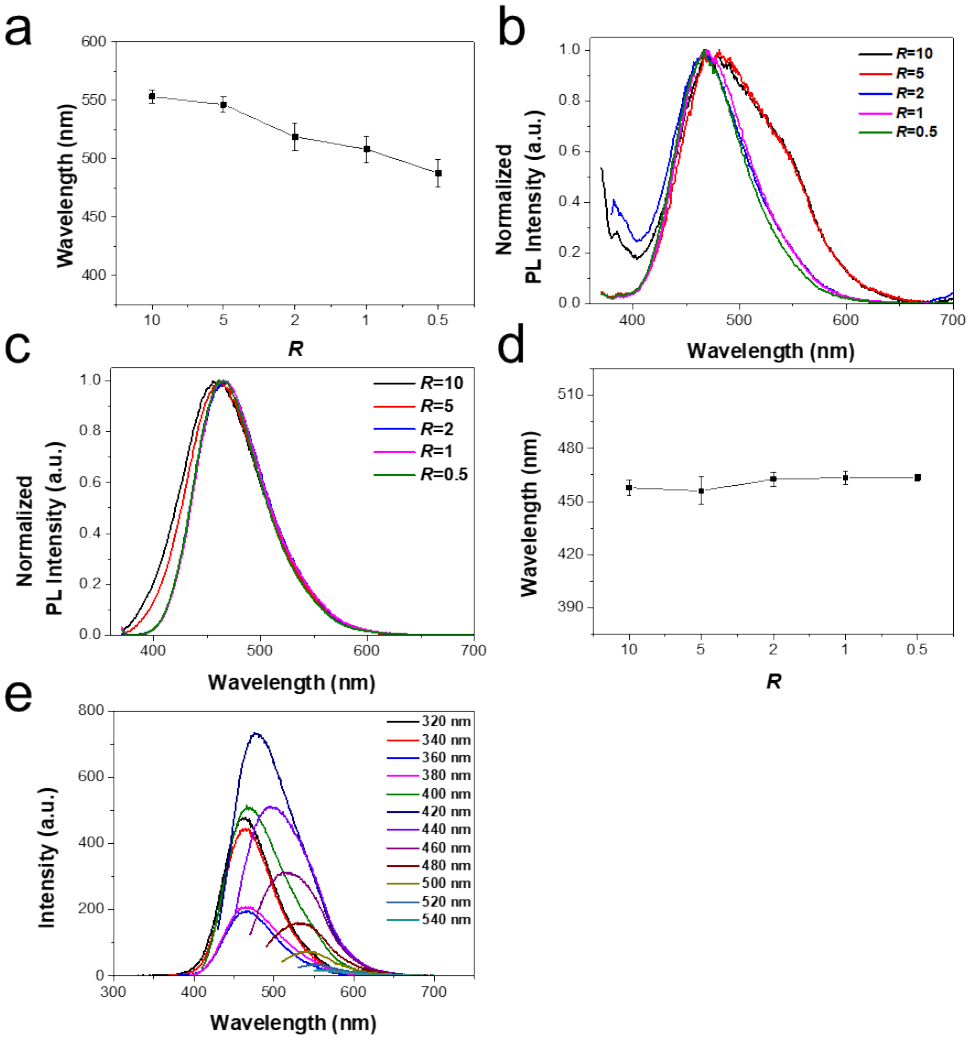

Figure S3. (a) The average peak values in PL spectra of hydrogels with thickness of ~ 2 mm. (b) The normalized PL spectra of the hydrogels with thickness of ~ 0.5 mm. (c) The normalized PL spectra of the CDs solutions after dialysis of hydrogels in water for 2 days. (d) The average peak values in the PL spectra of CDs solution after dialysis of hydrogels in water for 2 days. (e) The excitation-dependent PL spectra of CDs solution from hydrogel with *R*=2.

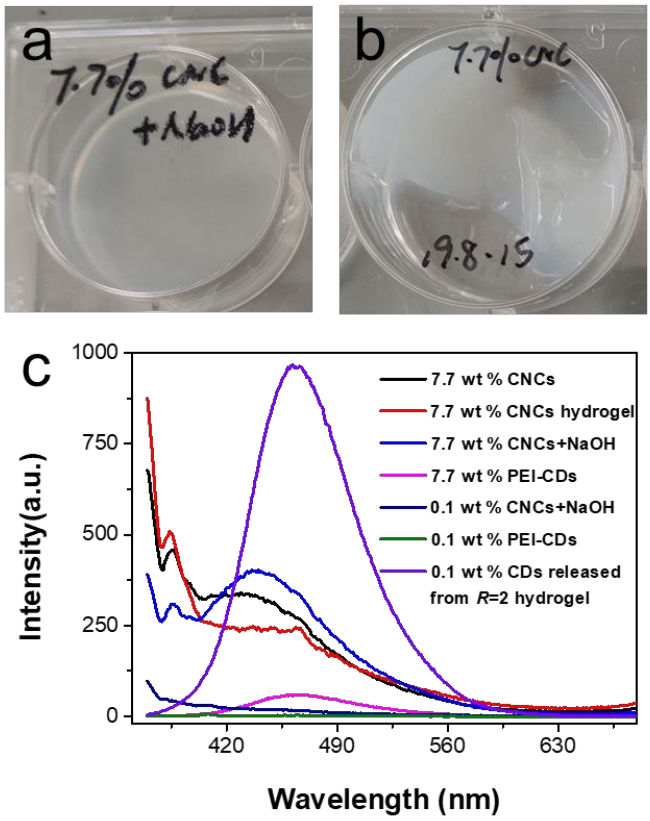

Figure S4. (a) Photograph of pure CNCs solution at pH of ~11 after hydrothermal treatment at 120 °C for 12 h. (b) Photograph of pure CNCs hydrogels. (c) The PL spectra of the 7.7 wt % CNCs, 7.7 wt % CNCs hydrogel, 7.7 wt % CNCs at pH of ~11 after hydrothermal treatment at 120 °C for 12 h, 7.7 wt % PEI-CDs, 0.1 wt % CNCs at pH of ~11 after hydrothermal treatment at 120 °C for 12 h, 0.1 wt % PEI-CDs, and 0.1 wt % CDs released from hydrogel of R=2 at λ_{ex} = 360 nm. The slit widths at excitation and emission were set as 3 nm and 5 nm, respectively.

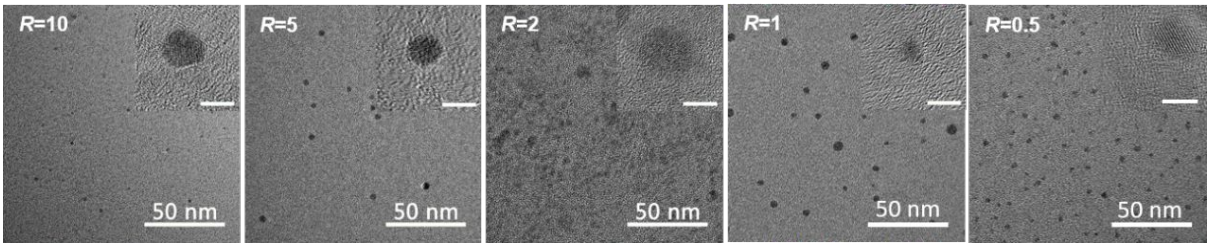

Figure S5. TEM images of CDs in the solution obtained by dialysis of hydrogels in water for 2 days. The scale bar in the inset is 5 nm.

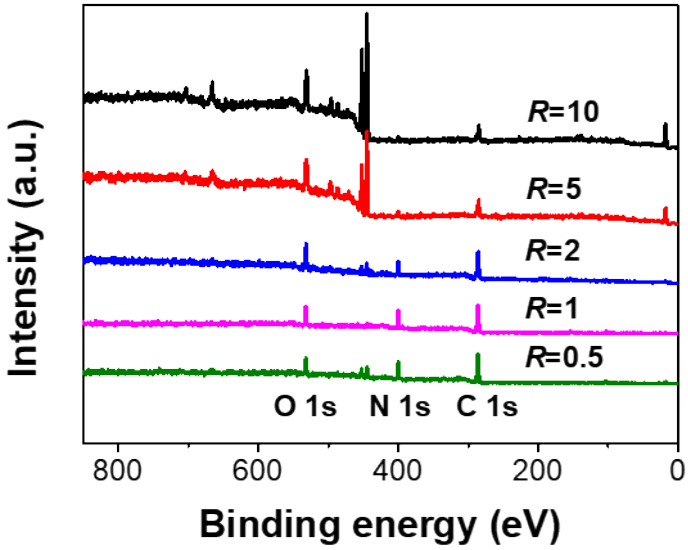

Figure S6. The XPS of the CDs obtained by dialysis of hydrogels in water for 2 days.

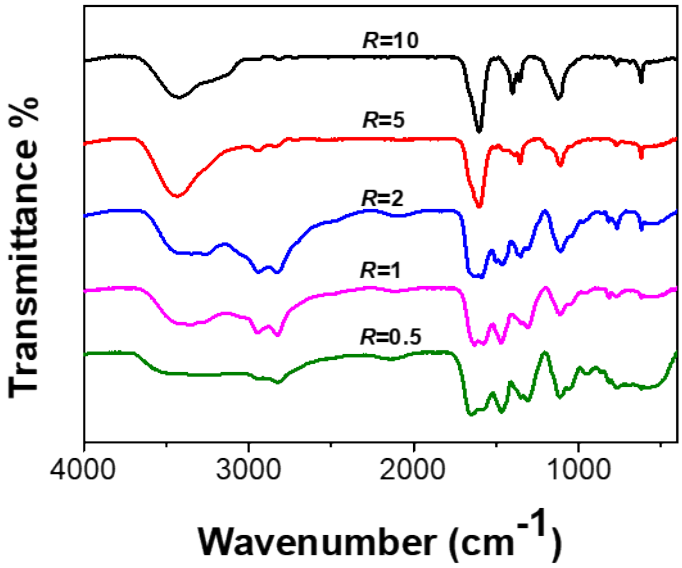

Figure S7. The FTIR spectra of CDs obtained by dialysis of hydrogels in water for 2 days.

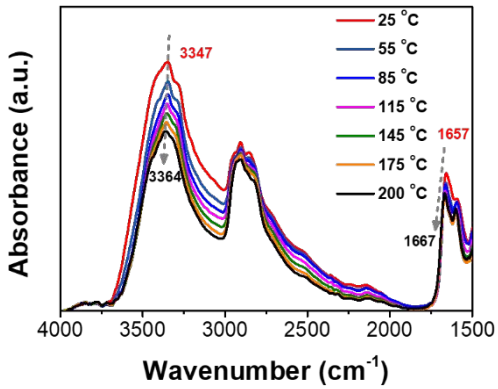

Figure S8. FTIR spectra of the hydrogel (*R*=2) with temperature in the range from 25 to 200 ^{o}C.

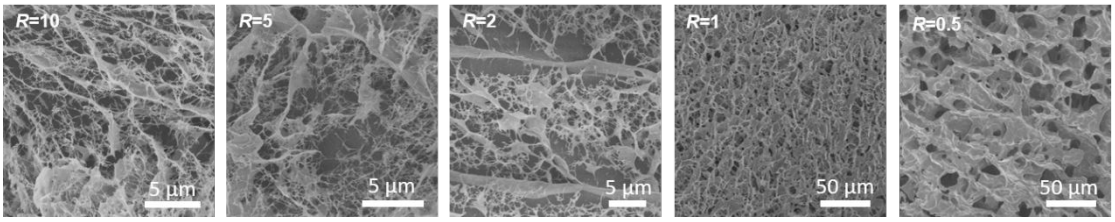

Figure S9. SEM micrographs of hydrogels at *R*=10, 5, 2, 1, 0.5, respectively.

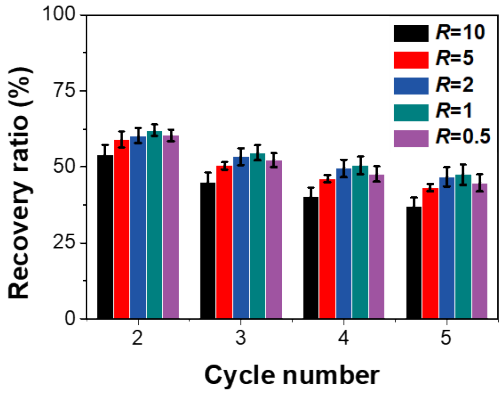

Figure S10. Recovery ratio of hydrogels with varying R and C_{total} = 7.7 wt % upon cyclic loading-unloading compressive tests.

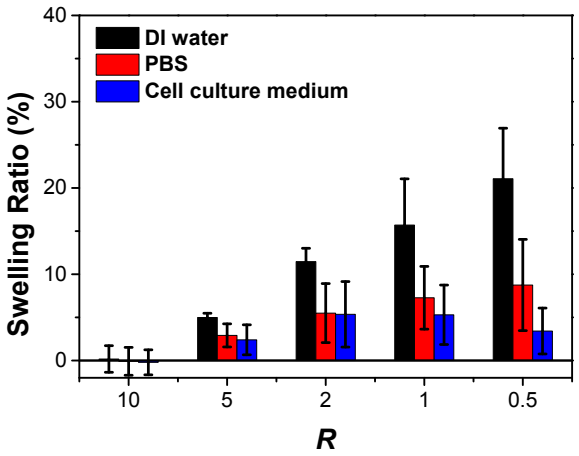

Figure S11. The swelling ratios of hydrogels in DI water, PBS, and cell culture medium respectively at room temperature.

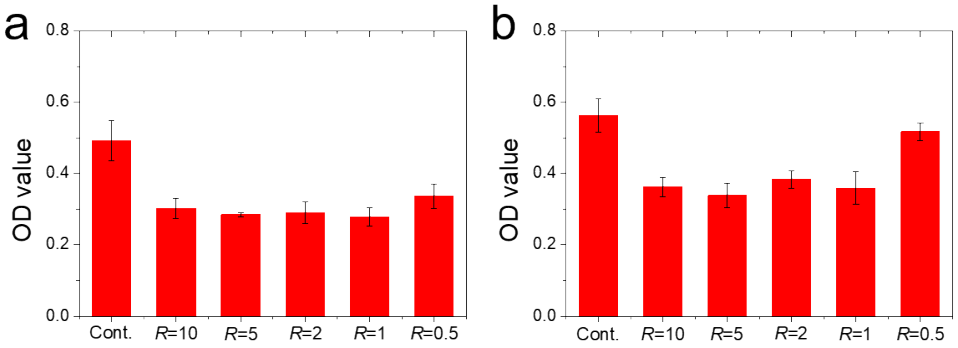

Figure S12. Cell proliferation of MC3T3-E1 (a) and CAL 27 (b) cell lines growth on the hydrogels for 1 day.

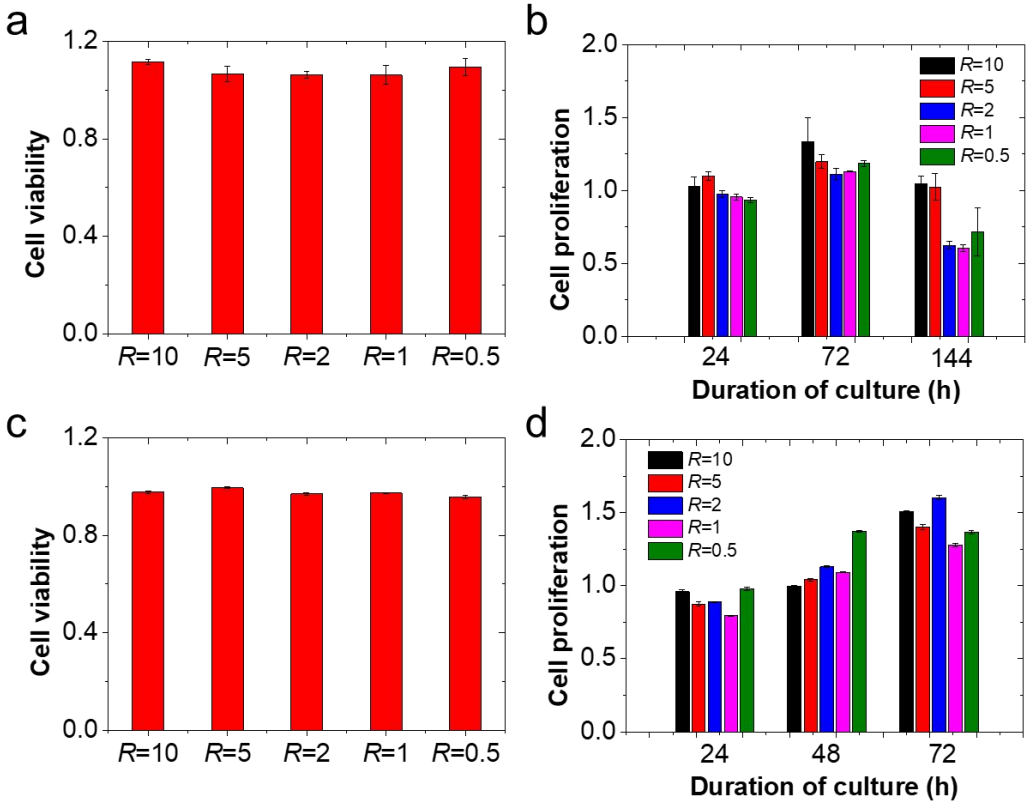

Figure S13. (a) Cell viability of MC3T3-E1 cells growth on the hydrogels on day 0 (6 hours after seeding cells). (b) Cell proliferation of MC3T3-E1 cells growth on the hydrogels. (c) Cell viability of MC3T3-E1 cells growth on the well plates in the present of the hydrogels in the cell culture medium on day 0 (6 hours after seeding cells). (d) Cell proliferation of MC3T3-E1 cells growth on the well plates in the present of the hydrogels in the cell culture medium.

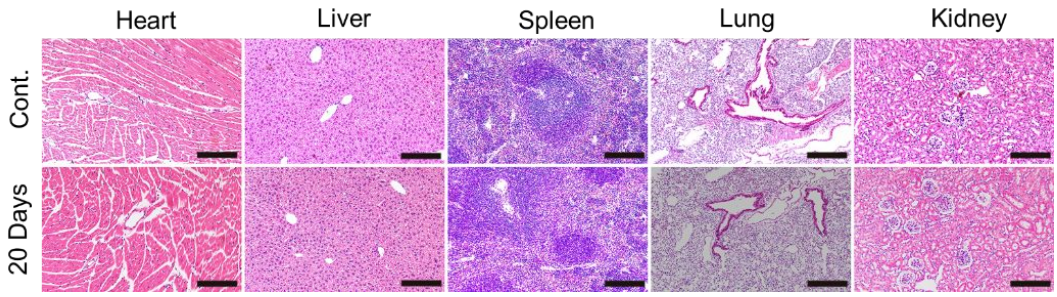

Figure S14. H&E staining of organs with hydrogels subcutaneous implantation of 20 days. The scale bar is 100 μm.

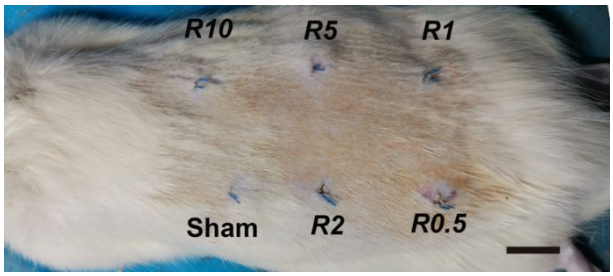

Figure S15. The subcutaneous implanted sites of the hydrogels in rat. The scale bar is 1 cm.